Available online at www.sciencedirect.com
ScienceDirect
Journal of the European Ceramic Society 30 (2010) 1015–1020
www.elsevier.com/locate/jeurceramsoc

Chemical composition and microstructure of Al_3BC_3 prepared by different densification methods

Sea-Hoon Lee [a,*], Hai-Doo Kim [a], Sung-Churl Choi [b], Toshiyuki Nishimura [c], Jin-Seok Lee [c], Hidehiko Tanaka [c]

[a] *Korea Institute of Materials Science, 531 Changwondaero, Changwon, Gyeongnam 641-831, Republic of Korea*
[b] *Department of Advanced Science and Engineering, Hanyang University, 17 Heangdang-Dong, Sungdong-Gu, Seoul 133-791, Republic of Korea*
[c] *National Institute for Materials Science, 1-1 Namiki, Tsukuba, Ibaraki 305-0044, Japan*

Received 10 May 2009; received in revised form 17 September 2009; accepted 28 September 2009

Abstract

"$Al_8B_4C_7$" and Al_3BC_3 powders were synthesized, and the formation of secondary phases was suppressed during the densification of the ternary aluminum borocarbides. The so-called "$Al_8B_4C_7$" was Al_3BC_3 containing excess Al and B. The excess components in "$Al_8B_4C_7$" promoted the densification of Al_3BC_3. The formation of secondary phases could not be controlled when using the reactive hot pressing method during the densification of Al_3BC_3. In contrast, monolithic Al_3BC_3 was obtained by separating calcination and hot pressing stage. The hardness, Young's modulus and fracture toughness of the sintered Al_3BC_3 were 13.9 GPa, 136 GPa and 2.2 MPa $m^{1/2}$, respectively.

Keywords: Calcination; Hot pressing; Carbides; Structural applications

1. Introduction

Al-rich aluminum borocarbides have been considered as promising candidates for lightweight structural application due to the unique combination of properties such as low density and high hardness.[1] In addition, the application field of the materials has been expanded to a sintering additive.[2] Consequently, intensive researches have been performed about the ternary materials during the last decades.[3,4]

The ternary compound was described as $Al_4B_{1-3}C_4$ by Matkovich et al. at 1964.[5] Inoue et al. reported that the $Al_4B_{1-3}C_4$ compound should in fact correspond to $Al_8B_4C_7$.[6] Since then, several tens of publications reported the phase until recently.[7–25] However, Hillebrecht and Meyer analyzed the structure of "$Al_8B_4C_7$" and reported that the correct molecular formula of the compound is Al_3BC_3.[26] Several papers have described the properties and structure of Al_3BC_3.[1,3,4,27–30] However, experimental evidences which clearly verify the correct ternary phase among the two systems have not been sufficiently provided.[30]

In spite of the increasing interest about the aluminum borocarbides, the densification method and mechanical properties of the compounds have been rarely reported. Recently, Li et al. obtained dense Al_3BC_3 using reactive hot pressing method.[30] However, the formation of secondary phases such as Al_4C_3 could not be efficiently suppressed. The secondary phases are highly undesirable because some of them react with humidity and may deteriorate the properties of the components after some time.[30]

In the present report, experimental evidences to verify the proper aluminum borocarbides were provided. The improvement of sintering method and some mechanical properties of the sintered materials were also reported.

2. Experimental procedure

Metal Al (Reagent grade, Koso Chemical Inc.), B_4C (Grade HD20, H.C. Starck), and C (carbon black, MA-600B, Mitsubishi Chem.) were used for the synthesis of the aluminum borocarbides. The raw powders having the stoichiometric composition of Al_3BC_3 or "$Al_8B_4C_7$" (molar ratio of Al:B:C = 3:1:3 or 8:4:7, termed 3Al–B–3C or 8Al–4B–7C, Table 1) were mixed in ethanol using an ultrasonifier for 10 min (US-1200T,

* Corresponding author. Tel.: +82 55 280 3344; fax: +82 55 280 3392.
E-mail address: seahoon1@kims.re.kr (S.-H. Lee).

0955-2219/$ – see front matter © 2009 Elsevier Ltd. All rights reserved.
doi:10.1016/j.jeurceramsoc.2009.09.027

Table 1
Chemical composition (wt%) of the stoichiometric and synthesized aluminum borocarbide powders.

	Al	B	C	O
Stoichiometric Al_3BC_3	63.3	8.5	28.2	0
Stoichiometric $Al_8B_4C_7$	62.9	12.6	24.5	0
Al_3BC_3 as-fabricated	62.4	8.4	27.7	0.35
$Al_8B_4C_7$ as-fabricated	60.1	12.1	25.7	0.73

Nissei, Tokyo, Japan, sonication condition: 20 kHz, 1200 W) and the mixed slurries were dried with stirring using a hot plate.

Dense specimens were prepared with changing the conditions of calcination. In condition 1, the 3Al–B–3C and 8Al–4B–7C were calcined at 1800 °C for 1 h in flowing Ar under moderate pressure (0.2 MPa). Immediately after the calcination step, the synthesized aluminum borocarbides were hot-pressed at 1850 °C for 1 h ("$Al_8B_4C_7$") or at 1875 °C for 2 h (Al_3BC_3) under 60 MPa pressure in flowing Ar (Fig. 1(a)). The sintering process was termed calcination–hot pressing method. The graphite molds used for hot pressing were sealed using a BN paste in order to minimize the vaporization of aluminum during calcination.[31] For comparison, part of the 3Al–B–3C was sintered using reactive hot pressing. The powder mixture was pressed under 40 MPa at 1850 °C without the calcination stage, and was sintered for 1 h in flowing Ar (condition 2, Fig. 1(b)). In condition 3, the 3Al–B–3C was calcined at 1800 °C for 2 h in Ar. The obtained powder was nearly X-ray pure Al_3BC_3. The ternary compound powder was crushed using a mortar in air and was hot-pressed at 1850 °C for 1 h under 40 MPa pressure (Fig. 1(c)).

The densities of the specimens were analyzed using Archimedes' method. The theoretical densities of Al_3BC_3 and "$Al_8B_4C_7$" used for the calculation of relative density was 2.66 and 2.69 g/cm^3, respectively.[8,30]

Chemical analysis of the Al_3BC_3 powder was performed using an inductively coupled plasma atomic emission spectrometry (analyzed components: Al and B, ICP-AES, Optima 3300DV, Perkin Elmer), infrared absorption method (analyzed component: C, CS 444-LS, Leco, St. Joseph, MI) and inert gas carrying melting-infrared absorptiometer (analyzed component: O, TC-600, Leco, St. Joseph, MI), respectively.

The phase compositions of the borocarbide powders and bulk specimens were analyzed using X-ray powder diffraction (XRD, JDX-3500, JEOL) with Cu Kα radiation. The microstructure and chemical composition of the sintered borocarbides were analyzed using scanning electron microscopy (SEM, JSM-6700F, JEOL) and energy dispersive spectroscopy (EDS, Phoenix, EDAX).

Young's modulus, hardness and fracture toughness of the dense specimens were measured using an ultrasonic tester (5072PR, Panametrics) and Vickers indenter (AVK-A, Akashi, loading condition: 10 kg, 15 s). Fracture toughness was calculated using the formula proposed by Anstis et al.[32]

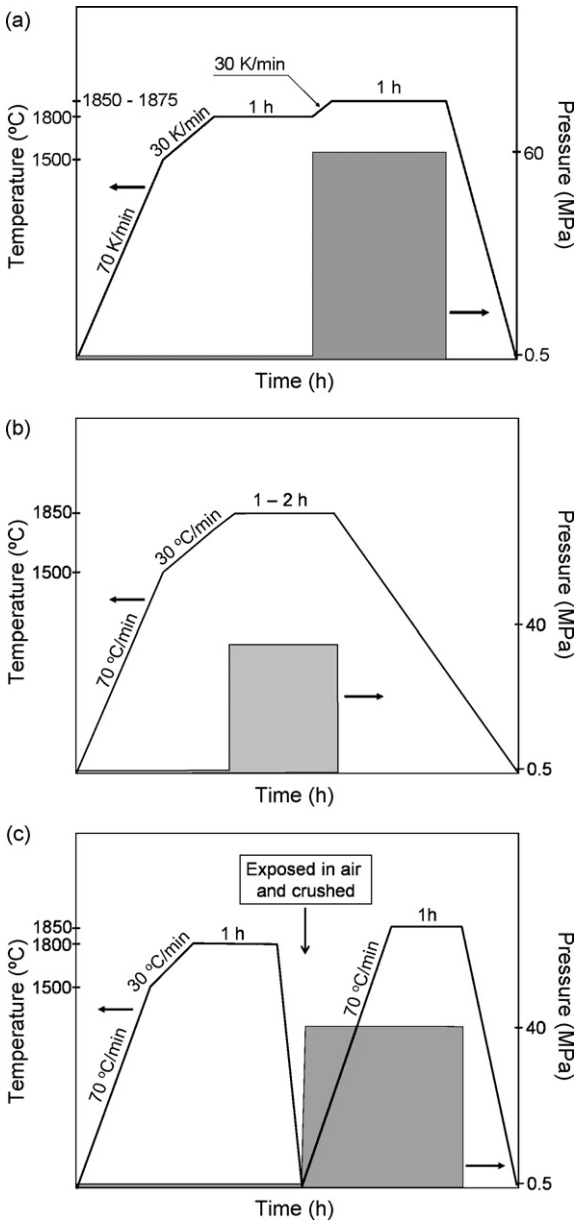

Fig. 1. Conditions of the heating rate and application of pressure: (a) condition 1, (b) condition 2 and (c) condition 3.

3. Results

Fig. 2 is the XRD data of Al_3BC_3 and "$Al_8B_4C_7$" reported in literatures and synthesized in this research. The X-ray reflections of Al_3BC_3 shown in Fig. 2(a) were calculated based on the crystal structure (space group: $P6_3/mmc$) reported in Refs. 1, 3. The calculated Al_3BC_3 peaks matched well with those of "$Al_8B_4C_7$" measured using a single crystal (Fig. 2(b)) except for the peak shift.[4]

The X-ray reflections of the synthesized Al_3BC_3 and "$Al_8B_4C_7$" powders (Fig. 2(c) and (d)) were similar with those obtained from a "$Al_8B_4C_7$" single crystal (Fig. 2(b)) except the small unidentified peaks at 28.4° and 36.9°. In spite of the large difference of chemical composition between Al_3BC_3

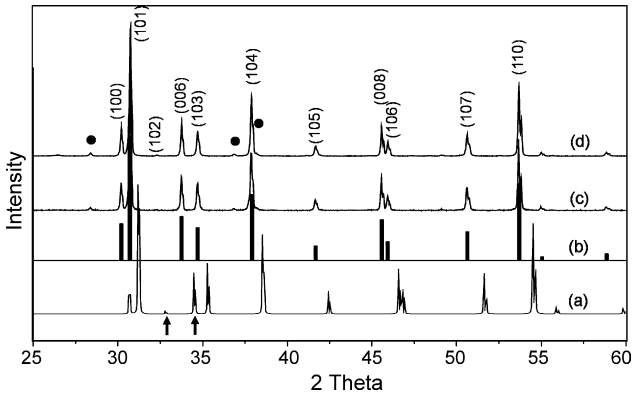

Fig. 2. XRD data of aluminum borocarbides. (a) Calculated reflections of Al_3BC_3 based on the data in Ref. 1 (calculated and added by one of the authors of Ref. 1, Z. Lin); (b) reflections of $Al_8B_4C_7$ reported by Inoue et al. measured from a single crystal (Ref. 6); (c) synthesized Al_3BC_3 powder and (d) synthesized "$Al_8B_4C_7$" powder: (●) unidentified peaks.

and "$Al_8B_4C_7$", the XRD data of both the powders were nearly identical.

Table 1 shows the chemical composition of the stoichiometric or synthesized aluminum borocarbide powders. The Al, B and C contents of the Al_3BC_3 powder were similar with the stoichiometric value. In contrast, a rather distinct reduction of Al content was observed in the synthesized "$Al_8B_4C_7$".

Fig. 3 illustrates the sintering shrinkage of the aluminum borocarbides above 1800 °C during calcination–hot pressing process. The shrinkage of the 8Al–4B–7C was nearly finished after sintering for 35 min at 1850 °C. In contrast, the densification of 3Al–B–3C continued for 1 h at 1875 °C. The relative density of Al_3BC_3 was lower than that of "$Al_8B_4C_7$" (97.7% *vs.* 98.1%, Table 2) although a higher temperature (1875 °C *vs.* 1850 °C) and longer holding time (2 h *vs.* 1 h) were applied for densification. In contrast, the shrinkage of the 3Al–B–3C powder was nearly finished after reactive hot pressing at 1850 °C for 40 min under 40 MPa pressure (condition 2, relative density: 98.9%). The densification of the crushed Al_3BC_3 powder was also nearly completed after hot pressing at 1850 °C using condition 3 (relative density: 99.1%).

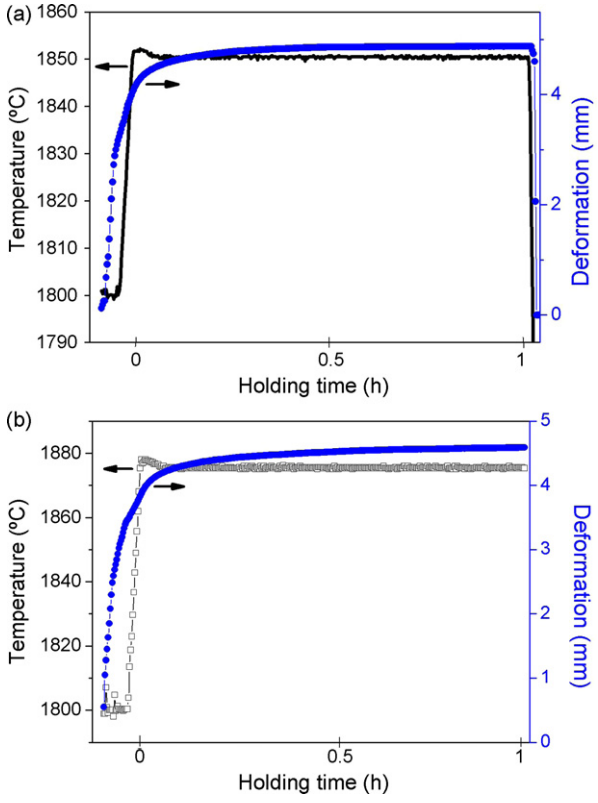

Fig. 3. Sintering shrinkage of (a) $Al_8B_4C_3$ at 1850 °C and (b) Al_3BC_3 at 1875 °C during hot pressing for 1 h under 60 MPa pressure in Ar.

Fig. 4 is the XRD data of Al_3BC_3 and "$Al_8B_4C_7$" sintered using the calcination–hot pressing method, which shows two differences from those of the powders. First, new peaks were observed at 26.4° and 38.4°, indicating the formation of C and Al during densification. Second, the intensity of peaks at 33.5° and 45.5°, which correspond to (0 0 6) and (0 0 8) plane, strongly increased after densification.[3,6] In addition, the specimens densified using conditions 2 and 3 contained secondary phases (Fig. 4(b) and (c)). The XRD data of Al_3BC_3 were similar with those of the "$Al_8B_4C_7$" after densification (Fig. 4(a) and (d)).

Fig. 5 is the microstructure and EDS data of the sintered Al_3BC_3 and "$Al_8B_4C_7$". The Al_3BC_3 grains had elongated morphology (Fig. 5(a)). The difference of the color in SEM figure indicated that the chemical composition of the grains was not identical. EDS analysis informed that the dark grains contained large amount of oxygen (Fig. 5(b) and (c)). The EDS peaks of B, C and Al were nearly identical at points 1–4.

In contrast to the uniform microstructure of Al_3BC_3, the sintered "$Al_8B_4C_7$" contained grains having irregular shape (Fig. 5(d)). EDS data indicated that the chemical composition of the elongated grains in "$Al_8B_4C_7$" was identical with that of Al_3BC_3, but the dark and irregular-shaped grains were mainly composed of B and Al (Fig. 5(e) and (f)). The results clearly indicated that "$Al_8B_4C_7$" is in fact Al_3BC_3 containing excess Al and B.

Table 2 summarized the mechanical properties of the sintered aluminum borocarbides. The Young's modulus and hardness

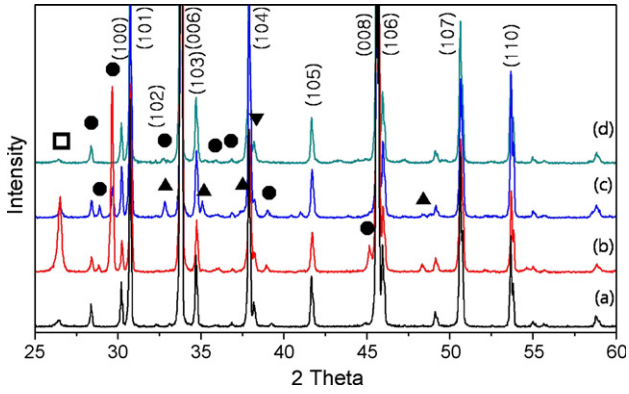

Fig. 4. XRD data of the dense aluminum borocarbides after hot pressing. (a) 3Al–B–3C, condition 1; (b) 3Al–B–3C, condition 2; (c) Al_3BC_3, condition 3; and (d) 8Al–4B–7C, condition 1: (□) graphite, (▼) aluminum, (▲) Al_4O_4C, (●) unidentified peaks, others: Al_3BC_3.

Table 2
Relative density and some mechanical properties of sintered aluminum borocarbides.

	Relative density/%	Young's modulus/GPa	Hardness/GPa	Fracture toughness/MPa $m^{1/2}$
Al_3BC_3	97.7	136	13.9	2.2
$Al_8B_4C_7$	98.1	161	14.1	2.2

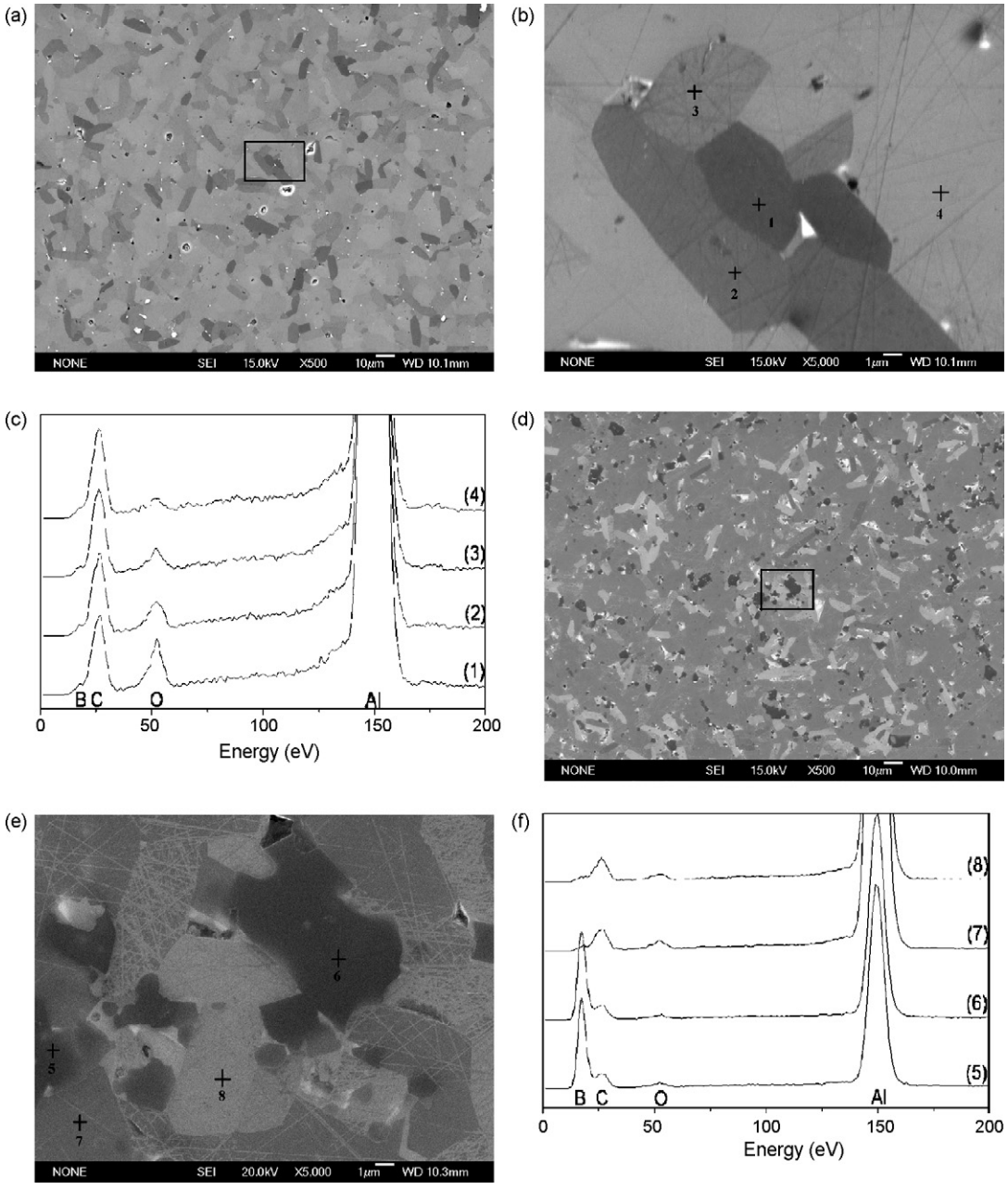

Fig. 5. Microstructure and EDS data of sintered samples: (a)–(c) Al_3BC_3; (d)–(f) $Al_8B_4C_7$.

of "$Al_8B_4C_7$" were higher than those of Al_3BC_3. The fracture toughness of the aluminum borocarbides was 2.2 MPa $m^{1/2}$.

4. Discussion

Different from the nearly stoichiometric Al_3BC_3 powder, the synthesized "$Al_8B_4C_7$" powder had a depletion of Al due to the vaporization of excess Al (Table 1). The generation of Al gas decreases strongly when Al forms carbides (*e.g.*, vapor pressure of molten Al: 291 Pa at 1527 °C, Al_4C_3: ~100 Pa at 1800 °C).[11,33] The aluminum-to-carbon ratio of stoichiometric Al_3BC_3 and "$Al_8B_4C_7$" is 2.24 and 2.57 by weight. While the ratio of the as-prepared "$Al_8B_4C_7$" decreased distinctly due to the vaporization of excess Al (2.34), that of the Al_3BC_3 powder

was nearly identical with the theoretical value (2.25). On the other hand, B content of the "$Al_8B_4C_7$" powder was similar to the stoichiometric value in spite of the excess because the vapor pressure of B is about five orders of magnitude lower than that of Al at 1800 °C.[11]

X-ray reflections of the "$Al_8B_4C_7$" powder did not show the presence of the excess components, the formation of secondary phases or the shift of peaks caused by the formation of a solid solution (Fig. 2(c) and (d)). The results indicated that most probably the excess Al and B within the "$Al_8B_4C_7$" powder formed an amorphous phase. The crystallization of amorphous B was reported to be suppressed by adding small amount of C.[34,35]

The change of the X-ray peak intensity of the sintered specimens at 33.5° and 45.5° (Figs. 2 and 4) was originated from the alignment of the elongated grains by the pressure applied during densification. The increase of the (0 0 6) and (0 0 8) peak intensity of the sintered Al_3BC_3 compared to those of the powders indicated that the c axis of the Al_3BC_3 grains were aligned perpendicular to the applied pressure. The preferential alignment of the elongated grains was clearly identified by SEM (Fig. 5(a)).

Al and C were formed in the sintered specimens due to the incomplete reaction (Fig. 4(c)) and/or the thermal decomposition of the ternary materials at and above 1850 °C. The melting temperature of "$Al_8B_4C_7$" was reported to be 1800–1850 °C.[12,18] However, the behavior did not occur at 1850 °C under 60 MPa pressure as shown in Fig. 3. Instead, the thermal decomposition of the ternary materials and the formation of Al and C began to occur during densification (Fig. 4). The onset temperature of decomposition of Al_3BC_3 is affected by the partial pressure of Al in the atmosphere.[36] In flowing Ar, the decomposition starts at 1400 °C, while the temperature shifted to ~1900 °C by using a sealed carbon mold in order to suppress the vaporization of Al.[36] In the present investigation, the raw powder mixture was placed in a sealed carbon mold, which effectively suppressed the decomposition of Al_3BC_3 and consequent formation of Al and C at 1850–1875 °C.

The densification of Al_3BC_3 was attained at 1850 °C by using the reactive hot pressing. However, the specimen contained large amount of carbon and secondary phases (Fig. 4(b)). The results indicated that the preparation of monolithic Al_3BC_3 by reactive hot pressing may be difficult although the method has a beneficial effect on the densification of Al_3BC_3.[30] Likewise, nearly complete densification could be achieved at 1850 °C when using the crushed Al_3BC_3 powder (condition 3). However, secondary phases such as Al_4O_4C were formed because the surface of the crushed Al_3BC_3 powder reacted with humidity to form aluminum oxides (Fig. 4(c)). The oxides are believed to promote the densification of Al_3BC_3 by forming a liquid phase because the eutectic temperature of Al_2O_3–Al_4O_4C is 1850 °C.[37] In contrast to the above results, monolithic Al_3BC_3 could be obtained by using the calcination–hot pressing method (Table 2, Fig. 4(a)). The above results indicated that the calcination–hot pressing method is the most effective among the tested conditions to obtain dense Al_3BC_3.

The densification of "$Al_8B_4C_7$" was easier than that of Al_3BC_3 (Fig. 3). Excess Al and B which were contained in "$Al_8B_4C_7$" presumably formed a liquid phase and promote the densification. The decomposition temperature of AlB_2 into a liquid and AlB_{12} was reported to be below 1200 °C.[38] The liquid phase in the sintered "$Al_8B_4C_7$" is believed to form the dark and irregular-shaped grains containing the excess constituents (Fig. 5(e)). The similarity of the XRD data between the sintered Al_3BC_3 and the "$Al_8B_4C_7$" (Fig. 4(a) and (d)) indicated that most probably the liquid phase did not crystallized during cooling down.

Wang et al. and Li et al. measured the mechanical properties of "$Al_8B_4C_7$" and Al_3BC_3, respectively.[8,30] The Young's modulus, hardness, and fracture toughness of the ternary materials were reported to be 137–163 GPa, 11.1–12.1 GPa and 2.3–3.9 MPa $m^{1/2}$, respectively.[8,30] The mechanical properties of the borocarbides measured in this research were similar to the reported values except for the high hardness (~14 GPa). The Young's modulus and hardness of "$Al_8B_4C_7$" was higher than those of Al_3BC_3 presumably because the relative density of the sintered "$Al_8B_4C_7$" was higher than that of Al_3BC_3 (98.1% *vs.* 97.7%).[39]

5. Conclusions

"$Al_8B_4C_7$" was Al_3BC_3 containing excess Al and B. The excess components remained as a secondary phase in the sintered specimens. The residual Al was partly removed by vaporization during the synthesis of "$Al_8B_4C_7$". The excess components promoted the densification during hot pressing. The formation of secondary phases could not be effectively suppressed when applying reactive hot pressing method. In contrast, dense Al_3BC_3 having homogeneous microstructure were obtained by using the calcination–hot pressing method. The Young's modulus and hardness of the sintered Al_3BC_3 were lower than those of "$Al_8B_4C_7$" presumably because of the remaining pores.

Acknowledgement

The kind discussion and help of Dr. Z. Lin were greatly appreciated.

References

1. Wang, J., Zhou, Y., Liao, T. and Lin, Z., First-principles prediction of low shear-strain resistance of Al_3BC_3: a metal borocarbide containing short linear BC_2 units. *Appl. Phys. Lett.*, 2006, **89**, 021917-1-3.
2. Lee, S. H., Tanaka, H. and Kagawa, Y., Spark plasma sintering and pressureless sintering of SiC using aluminum borocarbide additives. *J. Eur. Ceram. Soc.*, 2009, **29**, 2087–2095.
3. Jardin, C., Hillebrecht, H., Bauer, J., Halet, J. F., Saillard, J. Y. and Gautier, R., First-principles study of ternary metal boride compounds containing finite linear BC_2 units. *J. Solid State Chem.*, 2003, **176**, 609–614.
4. Wang, J., Zhou, Y., Lin, Z. and Liao, T., Pressure-induced polymorphism in Al_3BC_3: a first principles study. *J. Solid State Chem.*, 2006, **179**, 2739–2743.
5. Matkovich, V. I., Economy, J. and Giese Jr., R. F., Presence of carbon in aluminum borides. *J. Am. Chem. Soc.*, 1964, **86**, 2337–2340.
6. Inoue, Z., Tanaka, H. and Inomata, Y., Synthesis and X-ray crystallography of aluminum boron carbide, $Al_8B_4C_7$. *J. Mater. Sci.*, 1980, **15**, 3036–3040.
7. Tanaka, H. and Zhou, Y., Low temperature sintering and elongated grain growth of 6H-SiC powder with AlB_2 and C additives. *J. Mater. Res.*, 1999, **14**, 518–522.

8. Wang, T. and Yamaguchi, A., Some properties of sintered $Al_8B_4C_7$. *J. Mater. Sci. Lett.*, 2000, **19**, 1045–1046.
9. Zhang, X. F., Sixta, M. E. and De Jonghe, L. C., Grain boundary evolution in hot-pressed ABC–SiC. *J. Am. Ceram. Soc.*, 2000, **83**, 2813–2820.
10. Yoshida, K., Imai, M. and Yano, T., Microstructure and mechanical properties of hot-pressed silicon carbide fiber-reinforced silicon carbide composite. *Key Eng. Mater.*, 1999, **164–165**, 217–220.
11. Wang, T. and Yamaguchi, A., Synthesis of $Al_8B_4C_7$ and its oxidation properties in air. *J. Ceram. Soc. Jpn.*, 2000, **108**, 375–380.
12. Inomata, Y., Tanaka, H., Inoue, Z. and Kawabata, H., Phase relation in SiC–Al_4C_3–B_4C system at 1800 °C. *J. Ceram. Soc. Jpn.*, 1980, **88**, 353–355.
13. Tanaka, H., Nishimura, T., Hirosaki, N., Kishi, Y., Matsuo, H. and Ichikawa, Y., Low-temperature sintering of α- and β-SiC powders with AlB_2 additive. *Key Eng. Mater.*, 2006, **317–318**, 23–26.
14. Zhou, Y., Tanaka, H., Otani, S. and Bando, Y., Low temperature pressureless sintering of α-SiC with Al_4C_3-B_4C-C additions. *J. Am. Ceram. Soc.*, 1999, **82**, 1959–1964.
15. Lin, B. W., Imai, M., Yano, T. and Iseki, T., Hot-pressing of β-SiC powder with Al–B–C additives. *J. Am. Ceram. Soc.*, 1986, **69**, C67–C69.
16. Cairo, C. A. A., Graça, M. L. A., Silva, C. R. M. and Bressiani, J. C., Functionally gradient ceramic coating for carbon–carbon antioxidation protection. *J. Eur. Ceram. Soc.*, 2001, **21**, 325–329.
17. Chen, D., Sixta, M. E., Zhang, X. F., De Jonghe, L. C. and Ritchie, R. O., Role of the grain boundary phase on the elevated-temperature strength, toughness, fatigue and creep resistance of silicon carbide sintered with Al, B and C. *Acta Mater.*, 2000, **48**, 4599–4608.
18. Lukas, H. L., Aluminum–boron–carbon. In *Ternary Alloys*, *vol. 3*, ed. G. Petzow and G. Effenberg. VCH, Weinheim, 1990, pp. 140–160.
19. Kisly, P. S., Prikhna, T. A. and Golubyak, L. S., Properties of high-temperature solution-grown aluminum borides. *J. Less-Common Met.*, 1986, **117**, 349–353.
20. Moberlychan, W. J., Cao, J. J. and De Jonghe, L. C., The roles of amorphous grain boundaries and the β–α transformation in toughening SiC. *Acta Mater.*, 1998, **46**, 1625–1635.
21. Moberlychan, W. J. and De Jonghe, L. C., Controlling interface chemistry and structure to process and toughen silicon carbide. *Acta Mater.*, 1998, **46**, 2471–2477.
22. Yano, T., Budiyanto, K., Yoshida, K. and Iseki, T., Fabrication of silicon carbide fiber-reinforced silicon carbide composite by hot pressing. *Fusion Eng. Des.*, 1998, **41**, 157–163.
23. Dörner, P., Constitutional investigations on high temperature ceramics of the B–Al–C–Si–N–O system by means of thermochemical calculations, PhD Thesis, University of Stuttgart, Stuttgart, 1982, pp. 120–140.
24. Flinders, M., Ray, D., Anderson, A. and Cutler, R. A., High-toughness silicon carbide as armor. *J. Am. Ceram. Soc.*, 2005, **88**, 2217–2226.
25. Tanaka, H., Hirosaki, N., Nishimura, T., Shin, D. W. and Park, S. S., Nonequiaxial grain growth and polytype transformation of sintered α-silicon carbide and β-silicon carbide. *J. Am. Ceram. Soc.*, 2003, **86**, 2222–2224.
26. Hillebrecht, H. and Meyer, F. D., Synthesis, structure, and vibrational spectra of Al_3BC_3, a carbidecarboborate of aluminum with linear $(C{=}B{=}C)^{5-}$ anions. *Angew. Chem. Int. Ed. Engl.*, 1996, **35**, 2499–2500.
27. Rorl, P., *Phase Diagrams of Ternary Metal–Boron–Carbon Systems*. ASM International, Materials Park, OH, 1998, pp. 3–10.
28. Solozhenko, V. L., Solozhenko, E. G. and Lathe, C., Equation of state and thermal stability of Al_3BC. *Solid State Commun.*, 2006, **137**, 533–535.
29. Solozhenko, V. L., Meyer, F. D. and Hillebrecht, H., 300-K equation of state and high-pressure phase stability of Al_3BC_3. *J. Solid State Chem.*, 2000, **154**, 254–256.
30. Li, F., Zhou, Y., He, L., Liu, B. and Wang, J., Synthesis, microstructure and mechanical properties of Al_3BC_3. *J. Am. Ceram. Soc.*, 2008, **91**, 2343–2348.
31. Lee, S. H., Lee, J. S., Tanaka, H. and Choi, S. C., Al_3BC_3 powder—processing and synthetic mechanism. *J. Am. Ceram. Soc.*, in press.
32. Anstis, G. R., Chantikul, P., Lawn, B. R. and Marshall, D. B., A critical evaluation of indentation techniques for measuring fracture toughness. 1. Direct crack measurements. *J. Am. Ceram. Soc.*, 1981, **64**, 534–538.
33. Brandt, J. L., Properties of pure aluminum. In *Aluminum*, *vol. 1*, ed. K. R. van Hohn. American Society for Metals, Metals Park, OH, 1967, pp. 1–30.
34. Galasso, F., Vaslet, R. and Pinto, J., Formation of amorphous boron from the melt by rapid cooling. *Appl. Phys. Lett.*, 1966, **8**, 331–332.
35. Shalamberodze, S. O., Kalandadze, G. I., Khulelidze, D. E. and Tsurtsumia, B. D., Production of α-rhombohedral boron by amorphous boron crystallization. *J. Solid State Chem.*, 2000, **154**, 199–203.
36. Lee, S. H. and Tanaka, H., Thermal stability of Al_3BC_3. *J. Am. Ceram. Soc.*, in press.
37. Qiu, C. and Matselaar, R., Phase relations in the aluminum carbide–aluminum nitride–aluminum oxide system. *J. Am. Ceram. Soc.*, 1997, **80**, 2013–2020.
38. McHale, A. E. ed., *Phase Diagrams for Ceramists*, *vol. 10*. The American Ceramic Society, Westerville, OH, 1994, Fig. 8802.
39. Rice, R. W., *Porosity of Ceramics*. Marcel Dekker Inc., New York, 1998, pp. 73–74.